Lasers in Surgery and Medicine 21:444–455 (1997)

Intracranial Pressure Waves Generated by High-Energy Short Laser Pulses Can Cause Morphological Damage in Remote Areas: Comparison of the Effects of 2.1-μm Ho:YAG and 1.06-μm Nd:YAG Laser Irradiations in the Rat Brain

András Czurkó, MD, Zsolt Tóth, MD, Tamás Dóczi, MD, DSc, and Ferenc Gallyas, PhD, DSc*

Department of Neurosurgery, University Medical School of Pécs, Pécs, Hungary

Background and Objective: **Histological effects of 2.1-μm Ho:YAG and 1.06-μm Nd:YAG laser pulses were compared in the rat brain, with special regard to areas remote from the irradiated site.**
Study Design/Materials and Methods: **Laser pulses were delivered through a 0.6-mm glass fiber, the tip of which was either introduced into the caudate nucleus (application mode I), or held at a 2-mm distance above the exposed intact dura. In the latter case, the space between the dura and the fiber tip was filled either with physiological saline (application mode II) or with air (application mode III).**
Results: **In application modes I and II, but not in application mode III, Ho:YAG laser pulses of 1.5 J and 200 μs, but not Nd:YAG laser pulses with the same parameters, immediately caused morphological damage to a considerable number of neurons and axons randomly distributed among apparently normal ones in certain areas remote from the irradiated site. A decrease in the energy and an increase in the length of the pulses lowered the incidence of the remote morphological damage.**
Conclusion: **This novel finding may impose limits on the application of Ho:YAG lasers in human endoscopic neurosurgery. Lasers Surg. Med. 21:444–455, 1997.** **© 1997 Wiley-Liss, Inc.**

Key words: axonal damage; blood-brain barrier damage; endoscopic neurosurgery; light microscopy; neuronal damage

INTRODUCTION

Disregarding photodynamic therapy [1], two types of laser are most widely used in neurosurgery: the 1.06-μm-wavelength Nd:YAG laser, which is mainly absorbed by the blood [2], and the 10.6-μm-wavelength CO_2 laser, which is mainly absorbed by the tissue water [3]. The former is suitable for coagulation and for producing hemostasis and the latter for dissection and ablation [4].

It is a major disadvantage of the $C0_2$ laser that conduction of its beam through optic fibers is impractical. This makes its maneuverability poor,

Contract grant sponsor: OTKA; Contract grant numbers: T-16570, T-020287.

This work was performed in the context of the "MINOP" project of the German Ministry of Research and Development with the collaboration of Aesculap Meditec AG and the Department of Neurosurgery, University of Mainz, Germany.

*Correspondence to: Ferenc Gallyas, Ph.D., D.Sc., Section of Neuropathology, Department of Neurosurgery, University Medical School, Rét utca 2, H-7624 Pécs, Hungary.

Accepted 20 March 1997

its use in endoscopic surgery enormously difficult and its conduction through water impossible. Accordingly, several attempts have been made to replace this laser with others that are also mainly absorbed by tissue water (over 1.3 μm wavelength[3]). The 1.32-μm Nd:YAG laser [5], the 1.44-μm Nd:YAG laser [6], the 1.9-μm Nd:YAG laser [7], the 2.1-μm Ho:YAG laser [8], the 2.9-μm Er:YAG laser [9], and the 6.53-μm KTP laser [10] have been proposed for neurosurgical use so far.

The histopathologic effects on the nervous tissue of irradiation with all the above lasers have been extensively studied [1,4–6,8,10–13]. However, none of these studies reported on the presence of primary morphological damage in brain areas distant from the site of irradiation.

It has long been established that each high-energy, short laser pulse causes a microexplosion by rapidly converting the water in tissue fluids to steam at the site of absorption (acoustic effect [14]). The pressure waves generated by a round of such microexplosions may propagate deep into the target tissue. As reported previously [15,16], intracranial pressure waves generated by concussive head injuries immediately cause morphological damage to a number of neurons and axons even remote from the impact site. As a follow-up to observations obtained through the use of a blood-absorbed (1.06-μm Nd:YAG) and a water-absorbed (2.1-μm Ho:YAG) laser, the present study addresses the question of whether laser-generated pressure waves can also produce morphological damage in the central nervous tissue distant to the absorption site.

MATERIALS AND METHODS

The Laser Equipment

The experiments were carried out with an Aesculap-Meditec (Heroldsberg, Germany) custom-built laser apparatus capable of radiating 2.1-μm Ho:YAG- and 1.06-μm Nd:YAG laser pulses, either separately or simultaneously, through a 0.6-mm-thick glass fiber (laser fiber). The output energy was either 0.25 or 1.5 J per pulse for separate application and 0.75 J per pulse for each laser type when applied simultaneously. The pulse length was either 200 or 800 μs, while the pulse frequency was kept at 1 Hz. Either a single pulse or 10 consecutive pulses were delivered by setting a mechanical shutter into action. Pulse generation was started 1 min earlier than the application, in order to keep the pulse energy constant, as measured using an Ophir-Nova (Jerusalem, Israel) laser energy monitor. The free end of the laser fiber was fixed in a vertical position to the electrode holder of an LMIM (Budapest, Hungary) stereotaxic apparatus for rodents.

Animal Experiments

A total of 120 Wistar rats of either sex, weighing between 200 and 220 g, were anesthetized with i.p. pentobarbital (50 mg/kg) and fixed to the head holder of a stereotaxic apparatus. Thereafter, either a 1 mm^2 (application mode I) or a 3 mm^2 (application modes II and III) circular opening was drilled in the calvarium, with its center 2.5 mm lateral to the midline of the skull over the right hemisphere, either at the level of the bregma (application mode I) or 3 mm caudal to it (Application modes II and III).

Application mode I. In 81 animals, the dura was opened and the tip of the laser fiber was introduced into the core of the caudate putamen (0.0 mm with respect to the bregma, 2.5 mm lateral to the midline, and 3.5 mm deep under the dura).

Application mode II. In 18 animals a 2-cm-long plastic tube with a 1-cm inner diameter was tightly cemented to the calvarium, concentric with the craniotomy hole, and filled with physiological saline. The laser fiber, always pointing to the center of the craniotomy hole, was immersed in the physiological saline until its tip was approximately 2 mm above the intact dura.

Application mode III. In 21 animals, the laser fiber pointed to the center of the craniotomy hole and its tip was positioned 2 mm above the intact, air-dried dura.

Animals anesthetized with i.p. pentobarbital (50 mg/kg) were killed by transcardial perfusion of a fixative (25.7 g sodium cacodylate was dissolved in a mixture of 200 ml 20% paraformaldehyde and 800 ml distilled water, and the solution was then adjusted to pH 7.5 with hydrochloric acid) 1 min, 1 day, or 1 week following laser irradiation. The tested combinations of the varied parameters of the laser pulses, the application modes and the survival times are listed in Table 1. Each parameter combination was tested on three animals. Evans blue (4 ml/kg of a 2% solution) was administered intravenously to each animal with 1 min survival, 5 min before laser irradiation. Animals with parameter combinations 38, 39, and 40 served as sham-operated controls.

Tissue Processing

Brains, together with a 5-mm-long stub of the spinal cord were removed from the skull 24 hr after the start of fixation, immersed in the fixa-

TABLE 1. Tested Combinations of the Varied Parameters

Parameter combination serial no.	Laser pulse type	Application mode	Pulse number	Pulse energy J	Pulse length μs	Survival time
1	Ho	I	1	1.5	200	1 min
2	Ho	I	1	1.5	800	1 min
3	Ho	I	1	0.25	200	1 min
4	Ho	I	1	0.25	800	1 min
5	Ho	I	10	1.5	200	1 min
6	Ho	I	10	1.5	800	1 min
7	Ho	I	10	0.25	200	1 min
8	Ho	I	10	0.25	800	1 min
9	Ho	I	10	1.5	200	1 day
10	Ho	I	10	1.5	800	1 day
11	Ho	I	10	0.25	200	1 day
12	Ho	I	10	0.25	800	1 day
13	Ho	I	10	1.5	200	1 week
14	Ho	I	10	1.5	800	1 week
15	Ho	I	10	0.25	200	1 week
16	Ho	I	10	0.25	800	1 week
17	Ho	II	10	1.5	200	1 min
18	Ho	II	10	1.5	800	1 min
19	Ho	II	10	0.25	200	1 min
20	Ho	II	10	0.25	800	1 min
21	Ho	III	10	1.5	200	1 min
22	Ho	III	10	1.5	800	1 min
23	Ho	III	10	0.25	200	1 min
24	Ho	III	10	0.25	800	1 min
25	Nd	I	1	1.5	200	1 min
26	Nd	I	1	1.5	800	1 min
27	Nd	I	10	1.5	200	1 min
28	Nd	I	10	1.5	800	1 min
29	Nd	I	10	1.5	200	1 day
30	Nd	I	10	1.5	800	1 day
31	Nd	I	10	1.5	200	1 week
32	Nd	I	10	1.5	800	1 week
33	Nd	II	10	1.5	200	1 min
34	Nd	II	10	1.5	800	1 min
35	Nd	III	10	1.5	200	1 min
36	Nd	III	10	1.5	800	1 min
37	Ho/Nd	I	10	2 × 0.75	200	1 min
38	—	I	—	—	—	1 min
39	—	II	—	—	—	1 min
40	—	III	—	—	—	1 min

tive additionally containing 5.9 g $CaCl_2.2H_20$/l and serially frozen-sectioned either in the coronal or in the sagittal plane. Every tenth of a series of 60-μm-thick sections was stained by a recently elaborated silver technique that demonstrates traumatically-damaged neurons and axons without co-staining either the soma or appendages of normal neurons ("dark"-neuron method [17,18]). Adjacent sections were stained with 0.1% toluidine blue, dissolved in 1% acetic acid for the demonstration of both traumatically-damaged and normal neurons. Unstained sections were mounted on slides and covered with gelatin in order to examine the Evans-blue infiltration, which allows visualization of acute damage to the blood-brain barrier [19]. Long-persisting damage to the blood-brain barrier was assessed by the immunohistochemical demonstration of infiltrated serum globulins [20], using biotin-conjugated Sigma (St.Louis, MO) anti-rat IgG as primary antiserum and a Dako AB (Carpinteria, CA) Complex/HRP kit for visualization. Irreversible damage to axons was screened by means of an axon degeneration method [21], and confirmed by immunohistochemical staining of neurofilaments [22], through the use of a DAKO kit. Myelin degeneration was visualized by a silver method [23]. As an indirect sign of tissue damage, the hyperplasia and hypertrophy of microglial cells were demonstrated by using a silver technique [24].

RESULTS

Control Animals

In horizontal sections of the *control animals subjected to application mode I,* the stab wound made by insertion of the laser fiber into the brain was surrounded by two concentric ring-shaped damaged areas. The outer ring, with an outside diameter of about 1 mm, contained several neurons, including their dendrites, that stained black when using the silver method selectively demonstrating "dark" neurons (Fig. 1a). In toluidine blue preparations, hyperbasophilic and shrunken neurons were found in a similar arrangement. Evans blue infiltrated the inner ring-shaped area that did not contain silver-stained neurons (Fig. la). As demonstrated in sections stained first with toluidine blue (Fig. 1c) then, after being photographed, with silver (Fig. lb), the hyper-basophilic neurons were the same as those displaying injury-induced argyrophilia. However, inside the Evans blue-infiltrated area the argyrophilia of hyperbasophilic neurons partly or completely disappeared (Fig. lb,c). Neither "dark" neurons, nor Evans blue-infiltration, was observed in any further area. The other histological methods revealed no abnormality either within the ring-shaped zone of "dark" neurons or in any brain area remote from the stab wound.

The autopsy materials from the control animals subjected to application mode II or III (animals without a stab wound) were totally free of histopathologic signs detectable with any of the methods used.

Ho:YAG Laser; Application Mode I; 1-Min Survival

In animals receiving a single pulse of 1.5 J and 200 μs, the tip of the laser fiber was surrounded by an Evans-blue-infiltrated, quasi-spherical area of about 1.5 mm in diameter. In the sections stained either by the "dark"-neuron method or with toluidine blue, the Evans-blue-infiltrated area remained pale and was surrounded by an approximately 0.5-mm-thick zone containing numerous "dark" (silver-stained, hyperbasophilic and shrunken) neurons (Fig. 2a,b). On the other hand, in remote areas, several solitary "dark" neurons were found in the entorhinal cortex (Fig. 3a), the Purkinje cells in the cerebellum and the motor neurons in the thoracic spinal cord. In contrast with the dendritic tree, the axonal appendages of silver-stained cell bodies always remained unstained with silver. However, several solitary silver-stained axons were found in the pons and the cerebellar white matter (Fig. 3d), the cell bodies of which remained unstained with silver. Evans-blue infiltration was absent in remote areas.

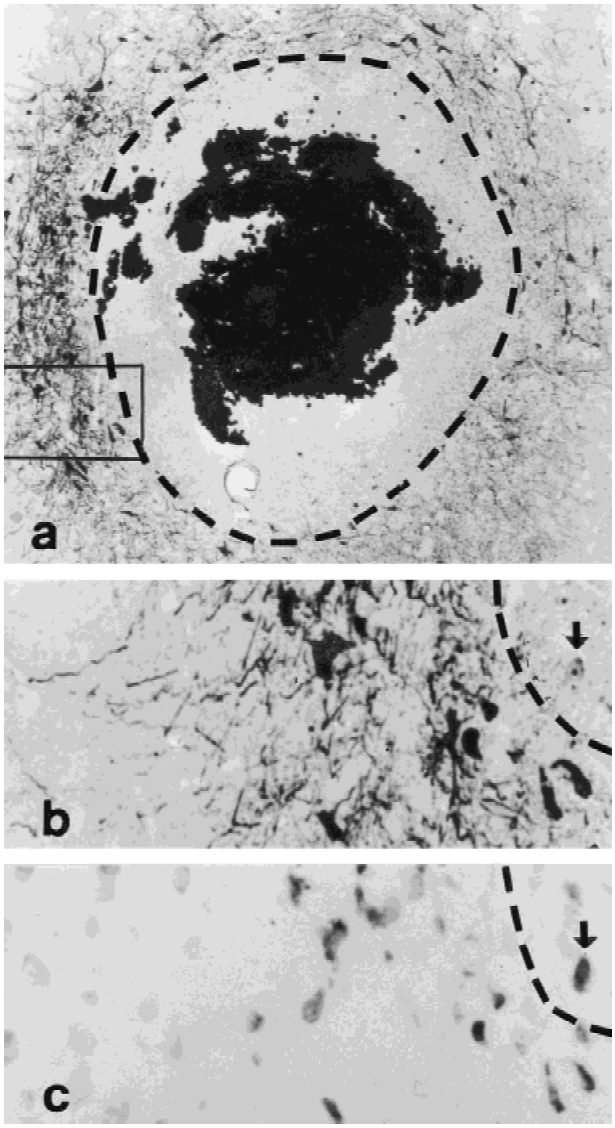

Fig. 1. Distribution of "dark" neurons around the stab wound made by insertion of the laser fibre into the brain. A 60-μm-thick horizontal section was stained first with toluidine blue **(c)** and, after being photographed, by the silver method for "dark" neurons **(a,b).** Dashed lines contours the Evans blue-infiltrated area. **b,c:** High-power magnifications of the area framed by continuous lines in a. Arrows in b and c point to a neuron which is hyper-basophilic with toluidine blue but only partly-stained with silver. Magnification ×60 in a and ×180 in b,c.

A decrease in energy to 0.25 J or an increase in length to 800 μs for the single pulse only slightly decreased the extent of the affected area around the tip of the laser fiber, but diminished the numbers of affected neurons and axons in remote areas considerably. For a combination of the

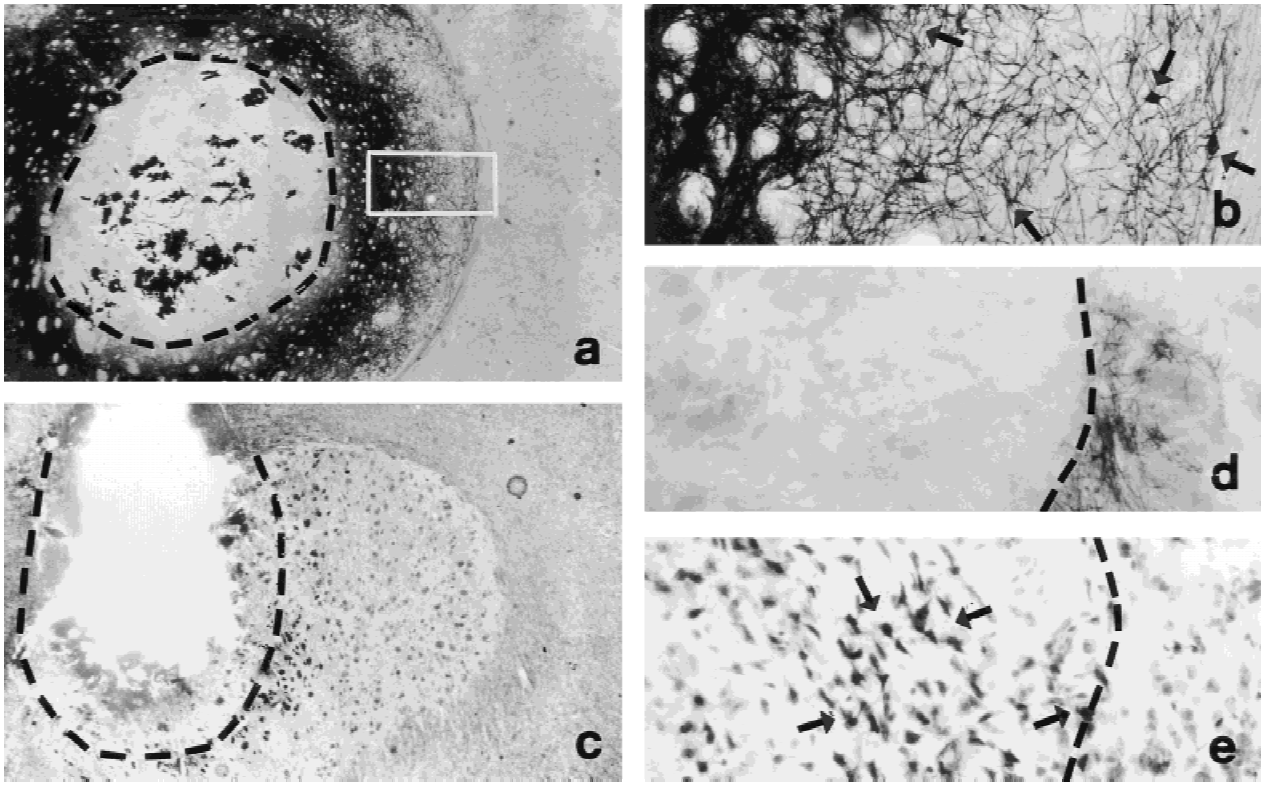

Fig. 2. Distribution of silver-stained "dark" neurons around the tip of the laser fibre in the caudate nucleus of rats that survived 1 min after having received a single Ho:YAG pulse (**a,b**), a single Nd:YAG pulse (**c**), or ten Ho:YAG pulses (**d**), in application mode I. Energy, length, and frequency of pulses were 1,5 J, 200 μs and 1 Hz, respectively. Dashed lines contours the Evans blue-infiltrated area. **b:** High-power magnification of the area framed by continuous lines in a. Arrows in b point to neuronal somata. **d,e:** Corresponding areas in consecutive sections stained with toluidine blue (e) and silver (d). Arrows in e point to neurons which are hyper-basophilic with toluidine blue but unstainable with silver. Sixty-μm-thick frontal sections. Magnification ×25 in a,c; ×180 in b; ×200 in d,e.

above values (0.25 J and 800 μs), both the diameter of the Evans-blue-infiltrated area and the width of the zone containing "dark" neurons appeared 20–30% smaller. On the other hand, no abnormalities were found in distant areas.

Ten consecutive pulses of 1.5 J and 200 μs increased the diameter of the Evans-blue-infiltrated area to about 2.5 mm. No silver-stained neurons, but several silver-stained dendrites, were found just outside this area (Fig. 2d). However, toluidine blue revealed numerous hyper-basophilic and shrunken neurons in a zone about 0.5 mm thick just inside its outline (Fig. 2e). In contrast, numerous silver-stained, hyperbasophilic and shrunken neurons were consistently found bilaterally, either in small groups or in a scattered distribution in the entorhinal cortex (Fig. 3b), cerebellum and thoracic spinal cord. Additionally, numerous silver-stained axon segments were consistently found bilaterally in the brain stem, pons, and cerebellar white matter (Fig. 3e), either in small bundles or randomly scattered. The numbers of the affected neuronal elements were considerably higher than those found with 1 single pulse (compare Fig. 3a and d with b and e). Outside these predilection areas, the rate of occurrence of either the neuronal or the axonal disturbance was much lower, especially in the contralateral hemisphere.

A decrease in the energy to 0.25 J or an increase in the length to 800 μs for ten consecutive pulses merely slightly reduced the extent of the affected area around the tip of the laser fiber but diminished the numbers of affected neurons and axons in remote areas considerably. For a combination of the above values (0.25 J and 800 μs), the diameter of the Evans-blue-infiltrated area decreased to about 2 mm. On the other hand, only a few instances of solitary neuronal or axonal disturbances were found even in the predilection areas.

Ho:YAG Laser; Application Mode I; 1-Day and 1-Week Survival

In the animals surviving for 1 day, independently of the energy and length of the laser

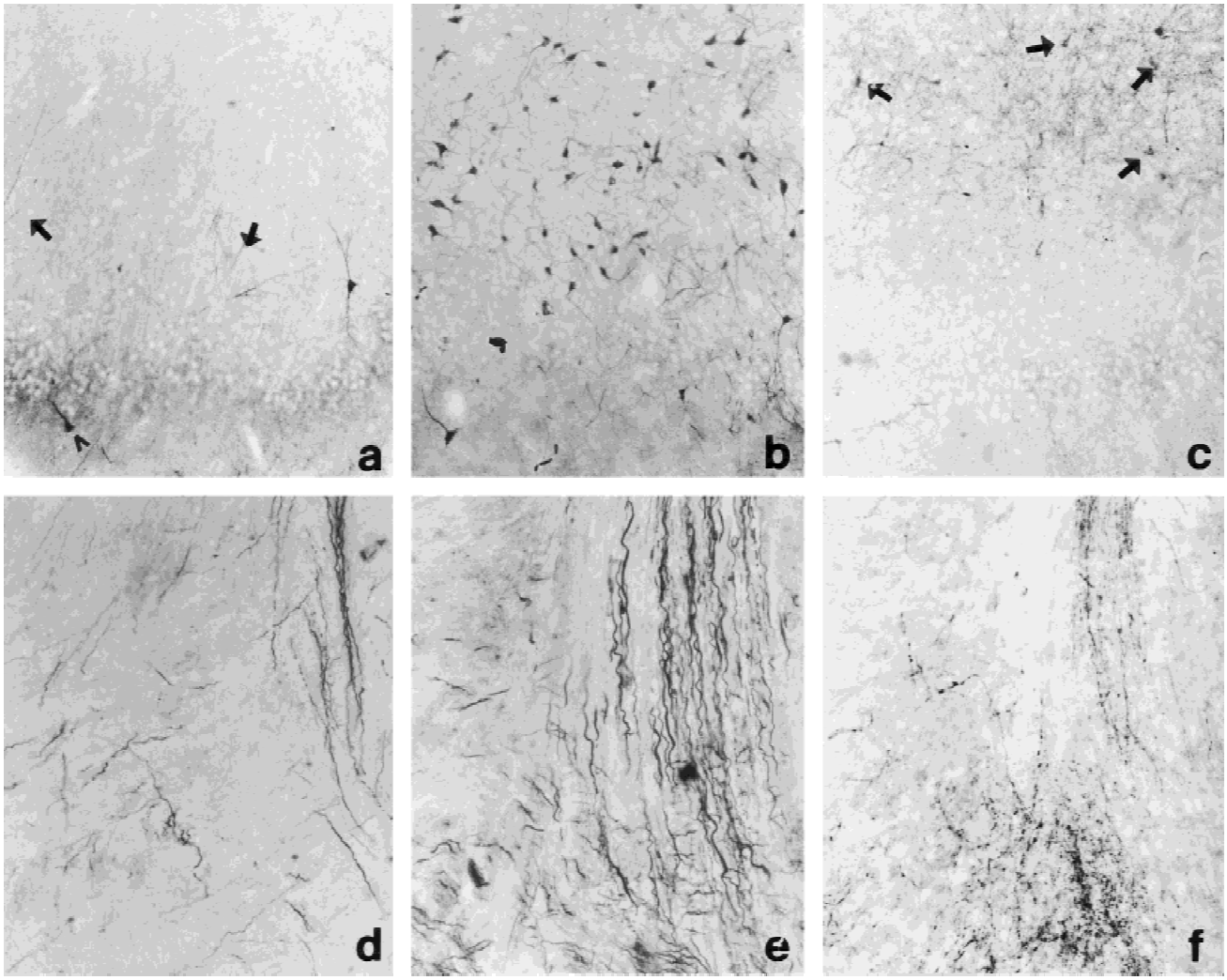

Fig. 3. Distribution of silver-stained "dark" neurons **(a–c)** and axons **(d–f)** in the rhinal cortex (a–c) and the cerebellar peduncles (e–f) of rats that survived 1 min (a,b,d,e) or 1 day (c,f) after having received 1 (a,d) or 10 (b,c,e,f) Ho:YAG pulses of 1.5 J, 200 μs, and 1 Hz, in application mode I. Arrows in (a) point to "dark" dendrites whose respective "dark" cell bodies were found in an adjacent section. An arrowhead in (a) indicates a "dark" neuron most dendrites of which were found in an adjacent section. Arrows in (c) point to neuronal cell bodies whose dendrites have disintegrated into droplets. In a–c, intact neurons are negatively stained. Sixty-μm-thick frontal sections. Magnification ×120 a–c and ×140 in d–f.

pulses, a quasi-spherical core of lacerated tissue structure (zone I) was surrounded by a relatively thick concentric zone with a slightly damaged tissue structure (zone II), which was surrounded by a relatively thin concentric zone with a severely damaged tissue structure (zone III). The outside diameter of the latter was similar to that infiltrated by Evans blue in the animals with a 1-min survival time. The whole lesion was infiltrated by serum globulins, while other brain areas were free of them. The concentric arrangement of the lesion was most clearly seen in myelin preparations (Fig. 4a). With toluidine blue, nerve cells were absent both from zones I and III, whereas in zone II "dark" and shrunken neurons were scattered among neurons that showed a pallor with respect to those found outside zone III. The "dark" neuron method did not stain any neurons either within, or in the close vicinity of, this concentric lesion. However, for 10 consecutive pulses of 1.5 J and 200 μs, the remote predilection areas contained several silver-stained neurons (Fig. 3c) and axons (Fig. 3f). The affected dendrites and axons were beaded or fragmented. Their number appeared much less than that of those found in the animals surviving for 1 min (compare Fig. 3b and e with c and f). In the toluidine-blue preparations, the soma of the silver-stained neurons was

shrunken and hyperbasophilic. No abnormalities were found in remote areas of animals irradiated with pulses of 0.25 J and 800 μs.

In the animals surviving for 7 days, the parenchymal lesion around the tip of the laser fiber appeared as large as in animals surviving for 1 day. Toluidine blue demonstrated no neurons inside the concentric lesion, whereas the myelin structure was still observable in zone II. This zone was densely packed with macrophages, while zone III was packed with microglial cells (Fig. 4b). Numerous microglial cells were found even outside the lesion (Fig. 4c), the farther, the less extensive. The silver method demonstrating "dark" neurons and axons did not stain any tissue element, either in the vicinity of the concentric lesion or in remote brain areas. The axon degeneration method revealed massive axonal disintegration in the vicinity of the lesion and along axon bundles coming from or passing through the lesion (e.g. the cortico-spinal tract). In addition to these tracts, mainly in the animals irradiated with 10 consecutive pulses of 1.5 J and 200 μs, this method demonstrated the bilateral disintegration of several solitary axons in the rhinal cortex (Fig. 5a) and parallel-running axons in the brain stem, pons, and cerebellar white matter (Fig. 5d). The presence of axonal disintegration in these areas was immunohistochemically confirmed in adjacent sections (Fig. 5b,e). In a similar localization, degeneration of individual myelin sheets and small foci of microglial proliferation (Fig. 5c,f) were also observed. No such abnormalities were detected in these brain areas of animals irradiated with pulses of 0.25 J and 800 μs.

Ho:YAG Laser; Application Mode II

In the animals surviving for 1 min, irradiation with 10 consecutive pulses of 1.5 J and 200 μs did not produce parenchymal lesions in the cortical area just under the tip of the laser fiber. However, the "dark"-neuron method stained several neurons in the dentate gyrus, hilus, and thalamus, whereas several "dark" axons in the subcortical white matter and the thalamus (Fig. 6). With toluidine blue, the affected neurons appeared hyperbasophilic and shrunken. Other brain areas, including those consistently affected in the case of application mode I, were free of abnormalities. In the animals irradiated with 10 consecutive pulses of 0.25 J and 800 μs even the hippocampus and the thalamus appeared unaffected.

In the animals surviving for 1 day, a slight

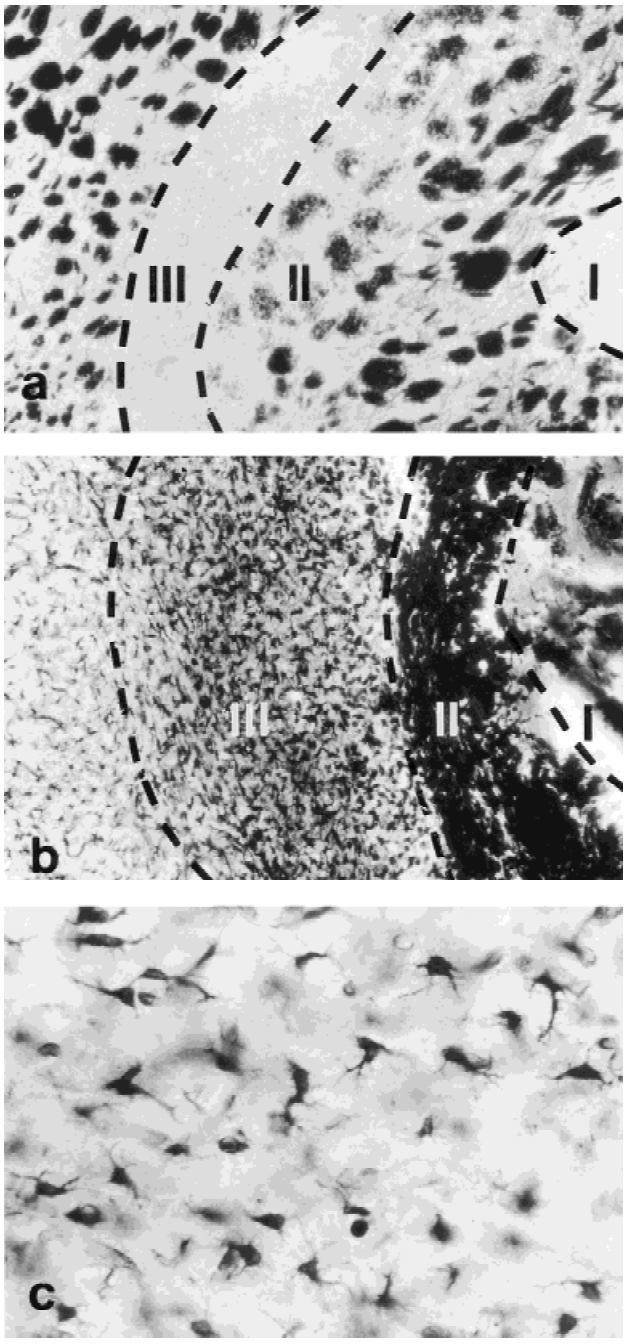

Fig. 4. Distribution of myelin (a) and microglial cells (b and c) in the caudate nucleus of rats that survived 1 day (a) or 1 week (b and c) after having received 10 Ho:YAG pulses of 1.5 J, 200 μs and 1 Hz, in application mode I. Note that stainability of myelin completely disappeared from zones I and III; zone II is densely filled with macrophages while zone III with microglial cells. **c:** High power magnification of an area in b, just outside zone III. Sixty-μm-thick frontal sections **(a and b):** ×50; **(c):** ×390

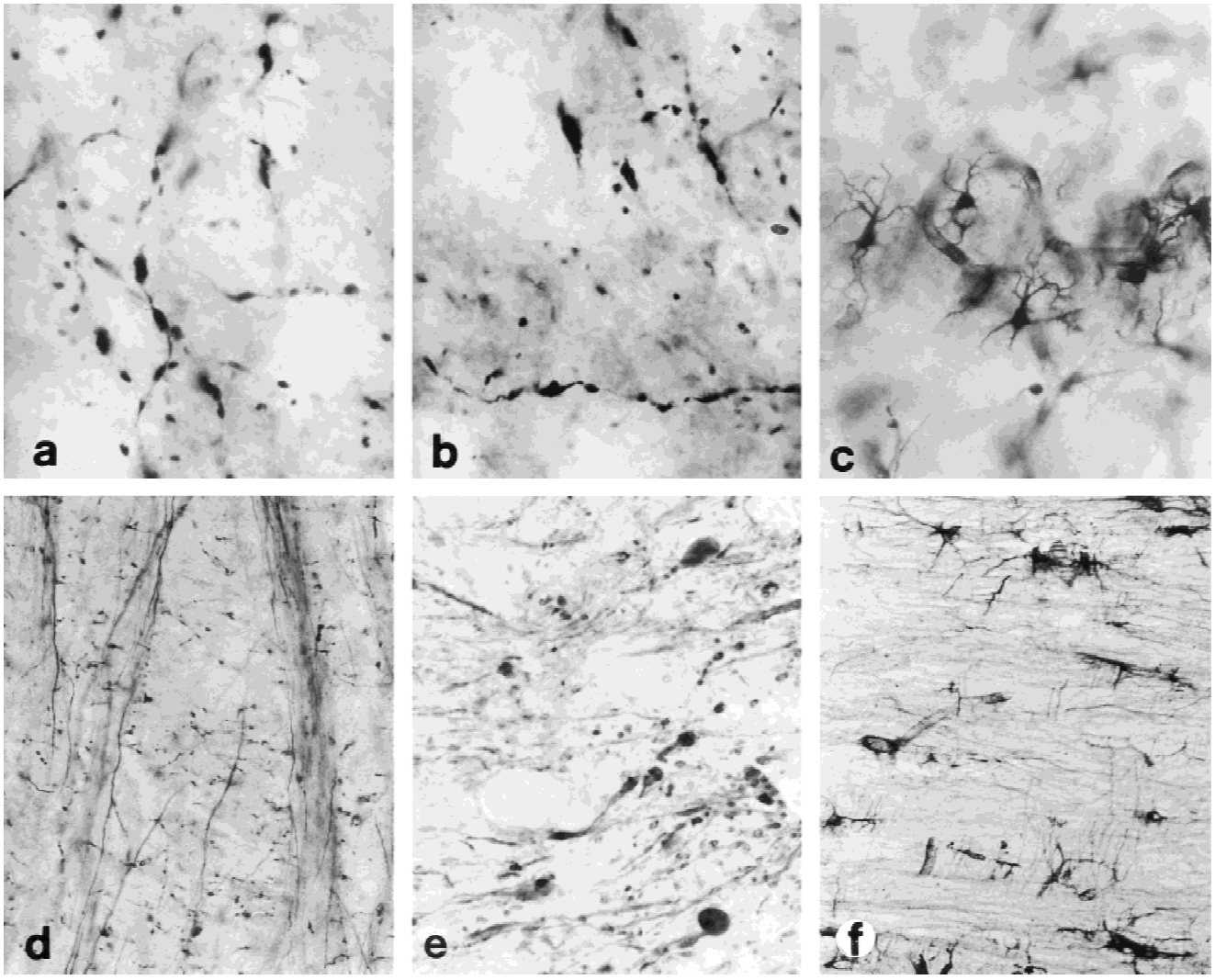

Fig. 5. Distribution of degenerating axons (a, b, d and e) and microglial cells (c and f) in the rhinal cortex (a-c) and cerebellar peduncles (d-f) of rats that survived 1 week after having received 10 Ho:YAG pulses of 1.5 J, 200 μs and 1 Hz, in application mode I. **(a and c):** silver method for degenerating axons, **(b and e):** immuno-cytochemical method for neurofilaments, **(c and f):** silver staining for microglial cells. Note that only horizontal running axons are disintegrated in *d* and *e*. Sixty-μm-thick frontal sections. **(a-c):** ×420 ; **(d-f):** ×280

macrophage infiltration was observed above, in and under the dura mater. At a pulse energy of 1.5 J and a pulse length of 200 μs, the ipsilateral subcortical white matter and the thalamus contained several disintegrated solitary axons, the dentate gyrus of the ipsilateral hippocampus contained a few solitary granule cells with disintegrated dendrites, and other brain areas displayed no abnormality.

Ho:YAG Laser; Application Mode III

In a dome-shaped area with its center under the tip of the laser fiber, each combination of laser pulse parameters and survival times produced the same histological picture as that found in the directly damaged area of animals exposed to application mode I. However, no abnormality was observed in remote areas, irrespective of the values of the varied parameters.

Nd:YAG Laser

Except for the presence of "dark" neurons, the histological appearance of the parenchymal lesion in the vicinity of the tip of the laser fiber was similar to that caused by Ho:YAG irradiation of the same parameter combination (Fig. 2c).

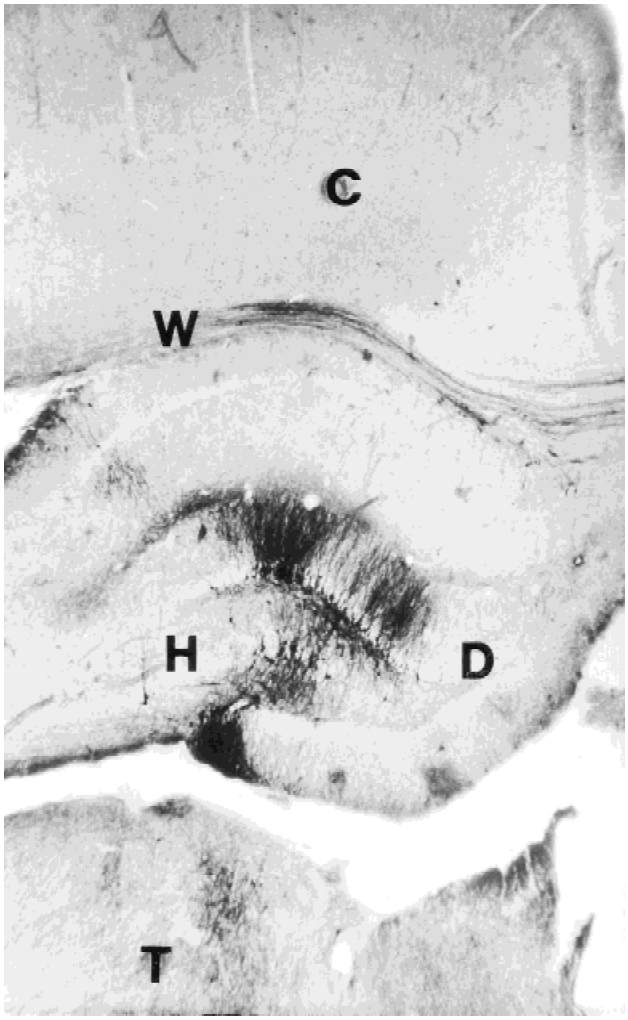

Fig. 6. Distribution of "dark" neurons and axons in the subcortical white matter (W), hippocampal dentate gyrus (D), hilus (H) and thalamus (T) of a rat that survived 1 min. after having received 10 Ho:YAG pulses of 1.5 J, 200 Fs and 1 Hz, in application mode II. Note that the neocortex (C) is free of damaged neurons and axons. Sixty-Fm thick frontal section. ×40

However, the sizes of the parenchymal lesions appeared to be 30–40% smaller, and there was a dome-shaped parenchymal lesion in the cortex even in animals subjected to application mode II.

As a significant difference from the effect of Ho:YAG pulses, the Nd:YAG pulses did not produce any remote neuronal or axonal damage in animals surviving for 1 min, irrespective of the application mode and the values of the other parameters. In long-surviving animals, only Wallerian degeneration, presumed secondary to the lesion in the vicinity of the tip of the laser fibre, was observed.

Simultaneous Application of Ho:YAG and Nd:YAG Lasers

Except for its size, which was slightly decreased, the parenchymal lesion in the vicinity of the tip of the laser fiber was similar to that caused by 10 consecutive Ho:YAG pulses of 1.5 J and 200 μs. In the remote predilection areas, both silver-stained neurons and axons were observed.

DISCUSSION

Morphological Damage Caused by Stabbing the Brain With the Laser Fiber

It has long been known that insertion of a needle into the brain, either in vivo or postmortem, immediately causes a number of neurons around the stab wound to undergo extensive shrinkage and to become hyper-basophilic (excessively stained with cationic dyes such as toluidine blue). There has been considerable dispute over the nature of such neurons that have traditionally been called "dark." Cammermeyer [25] proved that any kind of postmortem mechanical injury of the unfixed or improperly fixed brain produces "dark" neurons, but no "dark" neurons come about postmortem when the brains are left in the skull for 24 hours following transcardial perfusion with an aldehyde fixative. On the other hand, several later studies utilizing perfusion fixation and 24-hour delayed autopsy [15,16,18,26–28] have clearly demonstrated that "dark" neurons can be produced by mechanical injury of the brain also in vivo. To explain the "dual" genesis (both in vivo and postmortem) of "dark" neurons and certain other anomalous phenomena concerning them, one of the present authors earlier hypothesized a biomechanical mechanism of their formation [29].

Morphological Damage in the Vicinity of the Irradiated Site

With the exception of the features discussed in the following three paragraphs, the histological pictures in the vicinity of the tip of the laser fibre, and especially those observed in animals surviving for 1 day or 1 week, were very similar to those found by other authors who investigated the histological effects of laser lights of various wavelengths [l,4–6,8,10–13].

1) An inconsistency seems to exist between the two following observations: A single Ho:YAG laser pulse produces a large number of silver-stained neurons in the vicinity of the tip of the

laser fibre whereas a round of 10 pulses does not have the same effect. To solve this problem, we presume that substances released from barrier-damaged blood vessels can abolish the argyrophilia of the newly formed "dark" neurons. This reasoning is based on the presence of hyperbasophílíc and shrunken neuronal cell bodies in the outer zone of the area of damaged blood-brain barrier (Figs. lb,c and 2d,e). A similar phenomenon was observed in areas contused by concussive head injury [I6].

2) For application mode II, there is a fundamental discrepancy between the effects of Ho:YAG and Nd:YAG irradiation: The former does not produce a cortical lesion. The cause of it lies probably in the fact that the Ho:YAG pulses are absorbed by the physiological saline, present between the brain surface and the tip of the laser fiber, thus the released thermal energy is rapidly removed from the vicinity of the brain by convection. In animals subjected to application mode I or III, no such difference exists between the Ho:YAG and Nd:YAG laser pulses because both types warm up the tissue by being absorbed either in the tissue water or in the tissue blood.

3) The small number of animals (three) with the same parameter combinations does not allow any statistical analysis regarding the size of the lesion. Nevertheless, it can be stated that its dependence on the length, the energy, and the number of pulses in the ranges tested is highly underproportional. Regarding the two latter parameters, this is probably a consequence of the shortness of the heat relaxation time (i.e., the time needed for the heat to be conducted away by blood circulation [1]) as compared to the time between consecutive pulses.

Morphological Damage Remote From the Irradiated Site

For application mode I or II, the shrinkage and hyperbasophilia of neurons and the stainability with silver of both neurons and axons in certain remote areas of animals irradiated with high-energy short Ho:YAG laser pulses should be accepted as a manifestation of a morphological damage since histological signs of irreversible neuronal and axonal damage were present in the same remote areas of similarly-irradiated, long-surviving animals. In addition, there must be a causal relationship between the laser irradiation and such morphological damage, since the latter was consistently present following this insult, but invariably absent in the control animals. In principle, this relationship could reflect either a mechanical (direct), or a pathometabolic (indirect), causation. The pathometabolic causation could be mediated by laser-evoked systemic and/or local changes in the blood flow, blood gases, intracranial pressure, etc., and by a laser-evoked local release of metabolites from blood vessels and/or parenchymal cells. However, any indirect causation is contradicted by the fact that damaged neurons and axons were found in animals killed immediately after irradiation, before an indirect causation could become effective.

The existence of morphological damage in remote areas can be explained as follows: Absorption of each Ho:YAG laser pulse causes a microexplosion that generates a pressure wave penetrating deep into the tissue [14]. This results in local compressive, tensile, torsional, and/or shear deformations in the brain tissue [30], parameters of which may have different values, depending on the direction, amplitude, frequency, and/or damped oscillation of the pressure wave, the inhomogeneity and anisotropy of the brain viscoelasticity and the position of the irradiated site in respect to the skull, ventricles, main blood vessels, nerve tracts, etc. The topographic differences in the values of the deformation parameters may account for the topographic differences in vulnerability of neurons and axons. In this respect, the pattern of the predilection areas in Ho:YAG-irradiated animals subjected to application mode I may bear some relation to the shape of the posterior cranial vault. If this is true, the incidence of remote morphological damage may be much lower in animals with large brains.

High-energy short Nd:YAG pulses, in contrast with high-energy short Ho:YAG pulses, did not produce any morphological damage in distant brain areas. This is probably a consequence of the differences in the manner of their absorption, which determine the parameter values of the resulting pressure waves. The most obvious difference lies in the absorbing material (tissue water vs. red blood cells).

The dissimilarity between application modes II and III in producing remote neuronal and axonal damage can be explained by the assumption that the evaporated water can attain a much lower pressure if it can freely leave the site of laser pulse absorption than if it is trapped down by an abundant volume of physiological saline.

The small number of animals with the same parameter combinations does not allow a statistical analysis either of the rate of occurrence of

Ho:YAG-produced, or immediate neuronal and axonal damage in remote areas. However, it can be stated that the incidence of such neuronal damages considerably decreases with increasing pulse length or decreasing pulse energy and number, in the ranges tested. These findings are in accord with the assumption that the primary pressure at the site of absorption following each pulse is independent of the pulse number, but is enhanced both by increasing the pulse energy and shortening the pulse length.

A comparison of the incidence of the immediate signs with that of the chronic signs of remote morphological damage (Fig. 3) indicates that a considerable proportion of the immediately damaged neurons and axons might recover. Currently, the in vivo produced "dark" morphological state of cells is widely assumed to be a special pathway to the death of single cells, which displays some similarities to, but is probably different from, apoptosis [31,32]. However, a few authors have raised the idea that a proportion of "dark" neurons produced by ischemia [33], hypoglycemia [34], hyperosmotic shock [35], concussive head injury [16], poisoning with bicucculline [36], kainic acid [37], or flurothyl [38] may spontaneously recover.

Conclusions for Human Neurosurgical Practice

Thanks to the fiberoptic delivery system, laser irradiation is a promising weapon in the methodological armamentarium of endoscopic neurosurgery, permitting special treatments in brain areas difficult to access. However, the production of morphological damage in remote areas may impose certain limits on the endoscopic utilization of pulsed Ho:YAG lasers because the tip of the laser fiber is unavoidably surrounded by a medium with high water content. In principle, irradiation with any other water-absorbed laser pulses might also cause remote neuronal or axonal damage. On the other hand, as already mentioned, this kind of neuronal damage might be much milder in human brains. Until these issues have not been resolved, observance of the following appears to be reasonable: 1) the energy of individual pulses should be as low as possible, 2) the pulse length should be as long as possible, and 3) the number of delivered pulses should be as small as possible.

ACKNOWLEDGMENTS

This work was performed in the context of the MINOP project of the German Ministry of Research and Development with the collaboration of Aesculap Meditec AG and the Department of Neurosurgery, University of Mainz, and cosupported by grants from OTKA (T-16570 and T-020287).

REFERENCES

1. Edwards MSB, Boggan JE, Fuller TA. Review article: The laser in neurological surgery. J Neurosurg 1983; 59: 555–566.
2. Wharen RE Jr., Anderson RE, Scheithauer B, Sundt TM. The Nd:YAG laser in neurosurgery. Part I. Laboratory investigations: Dose-related biological response of neural tissue. J Neurosurg 1984; 60:531–539.
3. Bayly IG, Karth VB, Stevence WH. The absorption spectra of liquid phase H_20, HDO and D_20 from 0.7 μm to 10 μm. Infrared Physics 1963; 3:211–223.
4. Kuroiwa T, Tsuyumu M, Takei H, Inaba Y. Effects of Nd:YAG and $C0_2$ lasers on cerebral microvasculature. Study in normal rabbit brain. J Neurosurg 1986; 64:128–133.
5. Roux FX, Mordon S, Fallet-Bianco C, Merienne L, Devaux BC, Chodkiewicz JP. Effects of 1.32-μm Nd-YAG laser on brain thermal and histological experimental data. Surg Neurol 1990; 34:402–407.
6. Martiniuk R, Bauer JA, Mc Kean JD, Tulip J, Mielke BW. New long wavelength Nd:YAG laser at 1.44 μm: Effect on brain. J Neurosurg 1989; 70:249–256.
7. Steichen JD, Stewart, RB, Louis DN, Choi BB, Kung, R, Martuza RL. A new 1.9μm wavelength for neurosurgery. J Neurosurg 1989;73:611–614.
8. Ludwig HC, Bauer C, Behnke J, Fuhrberg P, Teichmann HP, Markakis E. Immuno-histochemical and electron microscopic effects of a new 2.1 micron Ho:YAG laser on the rat brain. Ann Acad Med Singapore 1994; 23:21–26.
9. McKenzie AL. An extension of the three zone model to predict depth of tissue damage beneath Er;Yag and Ho:YAG laser excision. Phys Med Biol 1989; 34:107–114.
10. Gamache FW Jr, Morgello S. The histopathological effects of the $C0_2$ versus the KTP laser on the brain and spinal cord: A canine model. Neurosurgery 1993; 32:100–104.
11. Brown TE, True C, McLaurin RL, Hornby P, Rockwell RJ. Laser radiation. Acute effect on cerebral cortex. Neurology 1966; 16:730–737.
12. Brown TE, True C, Mc Laurin RL Rockwell RJ, Hornby P. Laser radiation. II. Long-term effects of laser radiation on certain intracranial structures. Neurology 1970; 17: 789–796.
13. Eggert HR, Kiessling M, Kleihues P. Time course and spatial distribution of neodymium:yttrium-aluminium-garnet (Nd:YAG) laser-induced lesions in the rat brain. Neurosurgery 1985; 16:443–448.
14. Fine S, Klein E, Nowak W. Interaction of laser radiation with biological systems. I. Studies on interaction with tissues. Fed Proc 1965; 24(Suppl 14):535–547.
15. Gallyas F, Zoltay G. An immediate light microscopic response of neuronal somata, dendrites and axons to noncontusing concussive head injury. Acta Neuropathol 1992; 83:386–393.
16. Gallyas F, Zoltay G, Balás I. An immediate light micro-

scopic response of neuronal somata, dendrites and axons to contusing concussive head injury. Acta Neuropathol 1992; 83:394–401.
17. Gallyas F, Güldner FH, Zoltay G, Wolff JR. Golgï-like demonstration of "dark" neurons with an argyrophil III method for experimental neuropathology. Acta Neuropathol 1990; 79:620–628.
18. van den Pol AN, Gallyas F. Trauma-induced Golgi-like staining of neurons: A new approach to neuronal organization and response to injury. J Comp Neurol 1990; 296: 654–673.
19. Stroop WG, Battles EMM, Townsend JJ, Schaffer DC, Baringer JR, Straight RC. Porphyrin-laser photodynamic induction of focal brain necrosis. J Neuropath Exp Neurol 1989; 48:548–559.
20. Kiessling M, Herchenhan E, Eggert HR. Cerebrovascular and metabolic effects on the rat brain of focal Nd:YAG laser irradiation. J Neurosurg 1990; 73:909–917.
21. Gallyas F, Wolff SR, Böttcher H, Záborszky L. A reliable method for demonstrating axonal degeneration shortly after axotomy. Stain Technol 1980; 55:291–297.
22. Grady MS, Mclaughlin MR, Christman CW Volodka AB, Flinger CL, Povlishock JT. The use of antibodies targeted against the neurofilament subunits for the detection of diffuse axonal injury in humans. J Neuropathol Exp Neurol 1993; 52:143–152.
23. Gallyas F. Silver staining of myelin by means of physical development. Neurol Res 1979; 1:203–209.
24. Gallyas F, Hsu M, Buzsáki G. Four modified silver methods for thick sections of formaldehyde-fixed mammalian central nervous tissue: "dark" neurons, perikarya of all neurons, microglial cells and capillaries. J Neurosci Meth 1993; 50:159–164.
25. Cammermeyer J: The importance of avoiding "dark" neurons in experimental neuropathology. Acta Neuropathol 1961; 1:245–270.
26. Persson L, Hansson HA, Sourander P. Extravasation, spread and cellular uptake of Evans blue-labelled albumin around a reproducible small stab wound in the rat brain. Acta Neuropathol 1976; 34:125–136.
27. Queiroz LS, Eduardo RMP. Occurrence of dark neurons in living mechanically injured rat neocortex. Acta Neuropathol 1977; 38:45–48.
28. Stensaas SS, Edwards CQ, Stensaas LJ. An experimental study of hyperchromic nerve cells in the cerebral cortex. Exp Neurol 1972; 36:472–478.
29. Gallyas F, Zoltay G, Dames W. Formation of "dark" neurons of various origin proceeds with a common mechanism of biophysical nature. Acta Neuropathol 1992; 83: 504–509.
30. Gennarelli TA, Thibault LE. Biological models of head injury. In Becker D, Povlishock JT, eds. Central Nervous System Trauma Status Report. Richmond, VA: Byrd Press 1985, pp 391–404.
31. Harmon BV. An ultrastructural study of spontaneous cell death in mouse mastocytoma with particular reference to dark cells. J Pathol 1987; 153:345–355.
32. Wyllie AH. Apoptosis: Cell death in tìssue relations. J Path 1987; 153:313–316.
33. Kawai K, Nitecka L, Ruetzler CA. Global cerebral ischemia associated with cardiac arrest in the rat: I Dynamics of early neuronal changes. J Cereb Blood Flow Metab 1992; 12:238–249.
34. Auer RN, Kalimo H, Olsson Y, Siesjö BK. The temporal evolution of hypoglycemic brain damage. I. Light- and electron microscopic findings in the rat cerebral cortex. Acta Neuropathol 1985; 67:13–24.
35. Salahuddin TS, Kalimo H, Johansson BA, Olsson Y. Observations on exsudation of fibronectin in the brain after carotid infusion of hyperosmolar solutions. An immunohistochemical study in the rat indicating longlasting changes in the brain microenvironment and multifocal nerve cell injuries. Acta Neuropathol 1988; 76:1–10.
36. Atillo A, Söderfeldt B, Kalimo H, Olsson Y, Siesjö BK Pathogenesis of brain lesions caused by experimental epilepsy. Light and electron-microscopic changes in the rat hippocampus following bicucculline-induced status epilepticus. Acta Neuropathol 1983; 59:11–24.
37. Evans MC, Griffiths T, Meldrum BS. Kainic acid seizures and the reversibility of calcium loading in vulnerable neurons in the hippocampus. Neuropathol Appl Neurobiol 1984; 10:286–302.
38. Ingvar M, Morgan PF, Auer RN. The nature and tìming of excitotoxic neuronal necrosis in the cerebral cortex, hippocampus and thalamus due to flurothyl-induced status epilepticus. Acta Neuropathol 1988; 75:362–369.